Carcinogenesis vol.30 no.10 pp.1686–1695, 2009
doi:10.1093/carcin/bgp192
Advance Access publication August 3, 2009

Intercellular communication of cellular stress monitored by γ-H2AX induction

Jennifer S.Dickey*, Brandon J.Baird, Christophe E.Redon, Mykyta V.Sokolov, Olga A.Sedelnikova and William M.Bonner

Laboratory of Molecular Pharmacology, Center for Cancer Research, National Cancer Institute, National Institutes of Health, Bethesda, MD 20952, USA

*To whom correspondence should be addressed. Tel: 301 435 8668; Fax: 301 402 0752;
Email: dickeyj@mail.nih.gov
Correspondence may also be addressed to William M. Bonner.
Tel: 301 496 5942; Fax: 301 402 0752;
Email: bonnerw@mail.nih.gov

When cells are exposed to ionizing radiation (IR), unexposed cells that share media with damaged cells exhibit similar effects to irradiated cells including increased levels of DNA double-strand breaks (DSBs). Hypothesizing that this effect, known as the radiation-induced bystander effect, may be a specific instance of communication between damaged and undamaged cells regardless of damage source, we demonstrated that exposure of target cells to non-IR induces bystander damage in non-targeted cells as measured by γ-H2AX and 53BP1 focal formation. Initially, bystander damage was found primarily in S-phase cells, but at later times, non-S-phase cells were also affected. In addition, media from undamaged malignant and senescent cells also was found to induce DSBs in primary cultures. Media conditioned on cells targeted with either ionizing or non-IR as well as on undamaged malignant and senescent cells contained elevated levels of several cytokines. One of these, transforming growth factor beta (TGF-β), and nitric oxide (NO) were found to elevate numbers of γ-H2AX/53BP1 foci in normal cell cultures similar to levels found in bystander cells, and this elevation was abrogated by NO synthase inhibitors, TGF-β blocking antibody and antioxidants. These findings support the hypothesis that damage in bystander cells results from their exposure to cytokines or reactive compounds released from stressed cells, regardless of damage source. These results have implications for oncogenesis in that they indicate that damaged normal cells or undamaged tumor cells may induce genomic instability, leading to an increased risk of oncogenic transformation in other cells with which they share media or contact directly.

Introduction

In the radiation-induced bystander effect (RIBE), first described in 1992 (1), low doses of ionizing radiation (IR) result in cell survival fractions considerably lower than those expected from the fraction of cells that received radiation. Thus, irradiated cells appear to affect their unirradiated neighbors called bystander cells. Bystander cells exhibit effects similar to, but distinct from, those exhibited by exposed cells. These effects include point mutations, chromosomal abnormalities, micronuclei formation and apoptosis (2,3). Many of these outputs are accompanied by DNA damage in both bystander and irradiated cell populations (4), and staining for double-strand break (DSB) markers has indicated that DNA DSBs are present in bystander as well as in irradiated cells (5–8).

Since the RIBE was originally described, the purpose and extent of this effect has been an open question in the field. The ability of cells to transmit signals that promote genetic instability in neighboring cells seems both dangerous to the organism and pro-oncogenic. On the other hand, the bystander effect could serve to prepare cells for possible future stresses. We hypothesized that IR may not be the only cell-damaging agent that is capable of inducing a bystander effect (9). The cellular machinery required to induce the RIBE might also be used to transmit signals to neighboring cells following exposure to other forms of stress, both exogenous and endogenous. To examine if bystander effects occur in response to non-IR forms of stress, we used γ-H2AX and 53BP1 as a measure of DSB induction in bystander cells after subjecting targeted cells to a variety of damaging agents (10). Our findings indicate that the bystander effect may be a ubiquitous phenomenon and that this response to stress in neighboring cells may be an important pathway in the development of genomic instability and cancer progression.

Abbreviations: BrdU, bromodeoxyuridine; DSB, double-strand break; fpc, foci per cell; IR, ionizing radiation; NBF, normal breast fibroblast; NHF, normal human fibroblast; NO, nitric oxide; PAI-1, plasminogen activator inhibitor 1; PCNA, proliferating cell nuclear antigen; PrEC, prostate epithelial cell. RIBE, radiation-induced bystander effect; SDS, sodium dodecyl sulfate; UVA, ultraviolet A; UVC, ultraviolet C.

Materials and methods

Cell lines and culture

HeLa cervical adenocarcinoma (CCL-2; ATCC, Manassas, VA), T406 glioma (Marinpharm, Luckenwalde, Germany), human normal breast fibroblasts (NBFs, population doubling PD 11, a gift of Dr O. Aprelikova), human normal human fibroblasts (NHFs, a gift of Dr I. Horikawa) and primary prostate epithelial cells (PrECs, CC-2255; Cambrex, East Rutherford, NJ) were utilized. With the exception of PrEC, cells were grown in Dulbecco's modified Eagle's medium (Invitrogen, Carlsbad, CA) supplemented with 10–15% fetal bovine serum (Gemini Bio-products, Sacramento, CA). PrECs were grown in supplied medium according to manufacturer's instructions (Cambrex). All cultures were maintained in a humid atmosphere containing 5% CO_2. In order to analyze the effect of various stresses on DNA DSB formation, NHFs were cultured in the presence of 0.1 mg/ml sodium dodecyl sulfate (SDS) (Sigma, St Louis, MO) for various times. This concentration of SDS did not affect cell viability as seen by trypan blue staining (data not shown). Likewise, 0–10 μM diethylamine NONOate, 0–10 ng/ml recombinant transforming growth factor beta (TGF-β, both from Sigma), 10 μg/ml TGF-β antibody (Promega, Madison, WI) and 10 μg/ml bromodeoxyuridine (BrdU) antibody (BD Biosciences, San Jose, CA) were introduced into NHF cultures for DSB analysis.

Ultraviolet A induction of DNA DSBs

Cells were seeded onto LabTek II two-well chamber slides (Nunc, Naperville, IL) and allowed to grow to ∼80% confluence. The day before the experiment, BrdU (Sigma) was added to the cell medium to a final concentration of 10 μM and allowed to incorporate into cells overnight. Hoechst dye 33342 (10 μg/ml; Sigma) was added to the cell medium 20 min prior to the experiment. Following Hoechst incorporation, cells were washed with phosphate-buffered saline, and 200 μl of cold medium was added. Cells were placed on ice and aluminum foil was used to shield half of the cells. Ultraviolet A (UVA) light was generated with a Blak-Ray Longwave Ultraviolet Lamp (UVP, San Gabriel, CA). Cells were exposed for a total of 1 min to a final dose of 0.04 J/cm^2. Fresh media was then added and cells were allowed to incubate from 30 min to overnight before fixation. BrdU, Hoechst or this dose of UVA alone is sufficient to cause DNA breaks (11,12). Likewise, staining with both BrdU and Hoechst without UVA exposure does not cause DNA damage (supplementary Figure S1 is available at *Carcinogenesis* Online). Additionally, to control for possible UVA light reflection underneath the aluminum foil, a black barrier was used, which did not affect the results.

Ultraviolet C induction of DNA damage

Cells were seeded onto LabTek II two-well chamber slides as above. On the day of the experiment, cells were washed with phosphate-buffered saline and 200 μl of cold medium was added. Cells were placed on ice and aluminum foil was used to shield half the culture. Ultraviolet C (UVC) was generated with an UVLMS-30 EL Series 3UV Lamp (UVP). Cells were exposed to a variety of doses. Fresh media was then added and cells were allowed to incubate from 30 min to overnight before fixation. In experiments designed to test the effect of inhibitors and antioxidants on bystander effect propagation, 1 mM N^G-methyl-L-arginine (L-NMMA; Sigma), 4 μM 7-nitroindazole (7-NI; Sigma), 0.1 mM aminoguanidine hemisulfate (AG) or 50 μM tempol (a gift of Dr J. Mitchell) was added to the culture medium 1 h (L-NMMA and 7-NI), 2 h (AG) or 4 h (tempol) prior to irradiation (13).

Analysis of cellular senescence

Cells were seeded onto LabTek II two-well chamber slides as above and were fixed and stained for senescence-associated beta-galactosidase using the

Senescence Detection Kit from Cell Signaling (Beverly, MA) according to manufacturer's instructions.

Medium transfer bystander analysis

T75 flasks containing medium donor cell cultures that were 90–95% confluent were chosen. The harvested medium (15 ml) was filtered through a 0.22 μm MILLEX®GP filter (Millipore, Billerica, MA) and then added to recipient cultures. Controls for medium only and medium conditioned on recipient cell cultures overnight were included in each experiment. The medium recipient cultures were incubated for various times (30 min to 24 h) before fixation and analysis.

Immunocytochemistry and DNA DSB quantification

The γ-H2AX and 53BP1 staining was performed as described previously (14).

Antibodies used included anti-γ-H2AX rabbit antibody [1:500 custom made (14)], anti-γ-H2AX mouse antibody (1:500; Millipore) or anti-53BP1 rabbit antibody (1:500; Novus, Littleton, CO). For proliferating cell nuclear antigen (PCNA) and thymine dimer staining, cells were lysed in hypotonic buffer [10 mM Tris–HCl (pH 7.4) 2.5 mM $MgCl_2$, 1 mM phenylmethylsulfonyl fluoride and 0.5% Nonidet P-40 (NP-40)] and processed as described previously (15). Cells were incubated with anti-thymine dimer mouse antibody (1:100; Sigma) or anti-PCNA rabbit antibody (1:100; Abcam, Cambridge, MA) for 2 h. Secondary antibodies were either anti-rabbit or anti-mouse Alexa-488- or Alexa-555-labeled antibody (Molecular Probes, Eugene, OR). Slides were mounted with propidium iodide or 4′,5-diamidino-2-phenylinodole, dihydrochloride. Quantification of DNA DSBs, viewed as merged γ-H2AX/53BP1 foci, was performed by manual counting with a PCM2000 laser scanning confocal microscope (Nikon, Augusta, GA) using a ×100 objective. Foci were counted in ∼100 randomly chosen cells in at least three separate images. Alternatively, γ-H2AX intensity was determined using the Adobe Photoshop software package (Adobe Systems, San Jose, CA).

Western blotting

Western blotting analysis was performed as described previously (16). Briefly, cells were lysed in buffer containing 150 mM NaCl, 20 mM HEPES–NaOH (pH 7.4), 25% glycerol, 0.1 mM ethylenediaminetetraacetic acid, 0.2% NP-40, 10 mM NaF and complete protease inhibitor cocktail (Roche, Indianapolis, IN). The isolated proteins were boiled in SDS sample buffer and loaded onto 4–20% Tris–glycine pre-cast gels (Invitrogen). Separated proteins were transferred onto a polyvinylidene difluoride membrane (Invitrogen). For immunoblotting, the membranes were incubated with γ-H2AX mouse monoclonal antibody (1:500) or β-actin mouse monoclonal antibody (1:1000, both from Abcam). The blots were incubated with horseradish peroxidase-conjugated anti-mouse antibody (1:10 000; Amersham Bioscience, Piscataway, NJ). The blots were visualized by enhanced chemiluminescence western blotting detection reagents (Amersham Bioscience).

Enzyme-linked immunosorbent assay

Enzyme-linked immunosorbent assays were performed using either the human inflammation or the human obesity enzyme-linked immunosorbent assay strip assays from Signosis (Sunnyvale, CA) according to the manufacturer's protocols.

Statistical analysis

Statistical analysis was performed using the Student's *t*-test when comparing γ-H2AX intensity or focal numbers as well as for enzyme-linked immunosorbent assays. Analysis of numbers of cells containing >4 foci per cell (fpc) plus PCNA protein staining was performed using the Fisher's exact test. In all cases, a P value < 0.05 was considered statistically significant.

Results

DNA DSBs induced with non-IR lead to a DSB bystander response

DSBs can be generated by UVA light in cells grown in the presence of BrdU and incubated with Hoechst 33342 before exposure (11). In contrast to IR, UVA light can easily be blocked. Therefore, in order to examine bystander effects to DSB formation in the absence of IR, we designed a protocol in which half of a cell culture was shielded from exposure to UVA light with aluminum foil, whereas the other half was directly exposed (Figure 1A, top). The dose of UVA light was sufficiently low (0.04 J/cm^2) that no DNA DSBs were induced in directly exposed cells and no bystander effect was seen in the absence of BrdU and Hoechst (supplementary Figure S1 is available at *Carcinogenesis* Online). Increases in apoptosis have been seen in bystander populations after exposure of neighboring cells to 100 kJ/m^2 UVA (9). However, this was not seen in our system. After exposure, the cultures were incubated for various times and then processed for microscopic examination of DSBs (Figure 1). In order to substantiate that the lesion marked by a γ-H2AX focus is a DSB, cells were also stained for 53BP1 and foci positive for both γ-H2AX and 53BP1 were counted (17).

In NBFs, γ-H2AX/53BP1 foci formed in the directly irradiated half-culture become significantly different from controls at 3 h and 1 day and then disappear over 3–5 days (Figure 1A, upper bar graph, black bars). γ-H2AX/53BP1 foci were also found in the shielded bystander half-culture, but focal formation increased more slowly reaching a maximum 5-fold induction at 3 days after exposure (Figure 1A, upper bar graph, gray bars). This level of bystander γ-H2AX focus formation is comparable with that found in the RIBE (18,19). As an independent measure, total nuclear γ-H2AX intensity was examined by computer image analysis (Figure 1A, lower bar graph). The relative intensity level of γ-H2AX paralleled the numbers of γ-H2AX/53BP1 foci in both the exposed and the bystander half-cultures, with the bystander NBFs exhibiting a 3-fold induction of γ-H2AX levels over control cultures after 3 days. Thus, these results demonstrate that a substantial bystander effect can be seen without exposure to IR in NBF cultures.

In order to investigate the commonality of the bystander effect, we examined two other cell types, HeLa and primary PrECs, utilizing the same protocol. In the case of HeLa, the shielded bystander half-cultures exhibited a >3-fold increase in the numbers of γ-H2AX/53BP1 fpc 1 day after exposure (Figure 1B, upper graph) and a >4-fold increase in total γ-H2AX intensity (Figure 1B, lower graph). In addition, immunoblot analysis also revealed a noticeable increase in γ-H2AX levels in the bystander cultures compared with the directly irradiated (Figure 1B, right). However, in contrast to NBFs, HeLa cell cultures exhibited a further increase in total γ-H2AX intensity at 5 days after exposure in the shielded bystander half-culture due to large numbers of apoptotic cells with high levels of γ-H2AX staining that were absent from the directly exposed cultures (Figure 1B, bottom images).

PrECs, the third cell line examined with the UVA light protocol, also displayed a bystander response. The shielded bystander half-culture exhibited a 7-fold increase in the numbers of γ-H2AX/53BP1 fpc at 3 h after irradiation (Figure 1C). In contrast to bystander HeLa cultures, bystander PrEC cultures contained few apoptotic cells. However, they did contain many enlarged cells (Figure 1C, right bottom image), which stained positive for senescence-associated beta-galactosidase, indicating that bystander PrEC cultures respond in part by becoming senescent.

All three cell types examined in this protocol experienced substantial bystander effects in response to the UVA protocol. However, there was considerable variety in the timing and nature of the bystander response. The timing of the maximal increase in γH2AX/53BP1 fpc varied from 3 days post-exposure for NBFs to 3 h post-exposure for PrECs. Also the nature of the bystander response differed among the cell types, with bystander HeLa cultures exhibiting many apoptotic cells and bystander PrEC cultures exhibiting many senescent cells. These varied responses may highlight the difference between transformed and primary cell culture in responding to bystander stress signaling. Additionally, this variety in the timing and nature of bystander responses among different cell types may help explain seemingly contradictory findings reported in the literature (5–7,20,21).

Non-DSB-induced DNA damage generates DSBs in bystander cells

The UVA protocol (Figure 1) showed that IR is not necessary to generate bystander effects. While the UVA protocol as well as exposure to IR generate DNA DSBs, UVC light induces primarily cyclobutane dimers and few, if any, DSBs in exposed cells (22). Half-shielded NHF cultures were exposed to UVC light, incubated for various times and then stained for γ-H2AX and 53BP1 (Figure 2A, top). The unshielded half-culture 3 h after exposure to 100 J/m^2 exhibited γ-H2AX pan-staining as expected (23) but lacked detectible γ-H2AX/53BP1 foci (Figure 2A, middle column). In contrast, the shielded bystander half-culture exhibited γ-H2AX/53BP1 foci and no pan-staining (Figure 2A, right column). The presence of cyclobutane dimers in the exposed half-culture and their absence in the

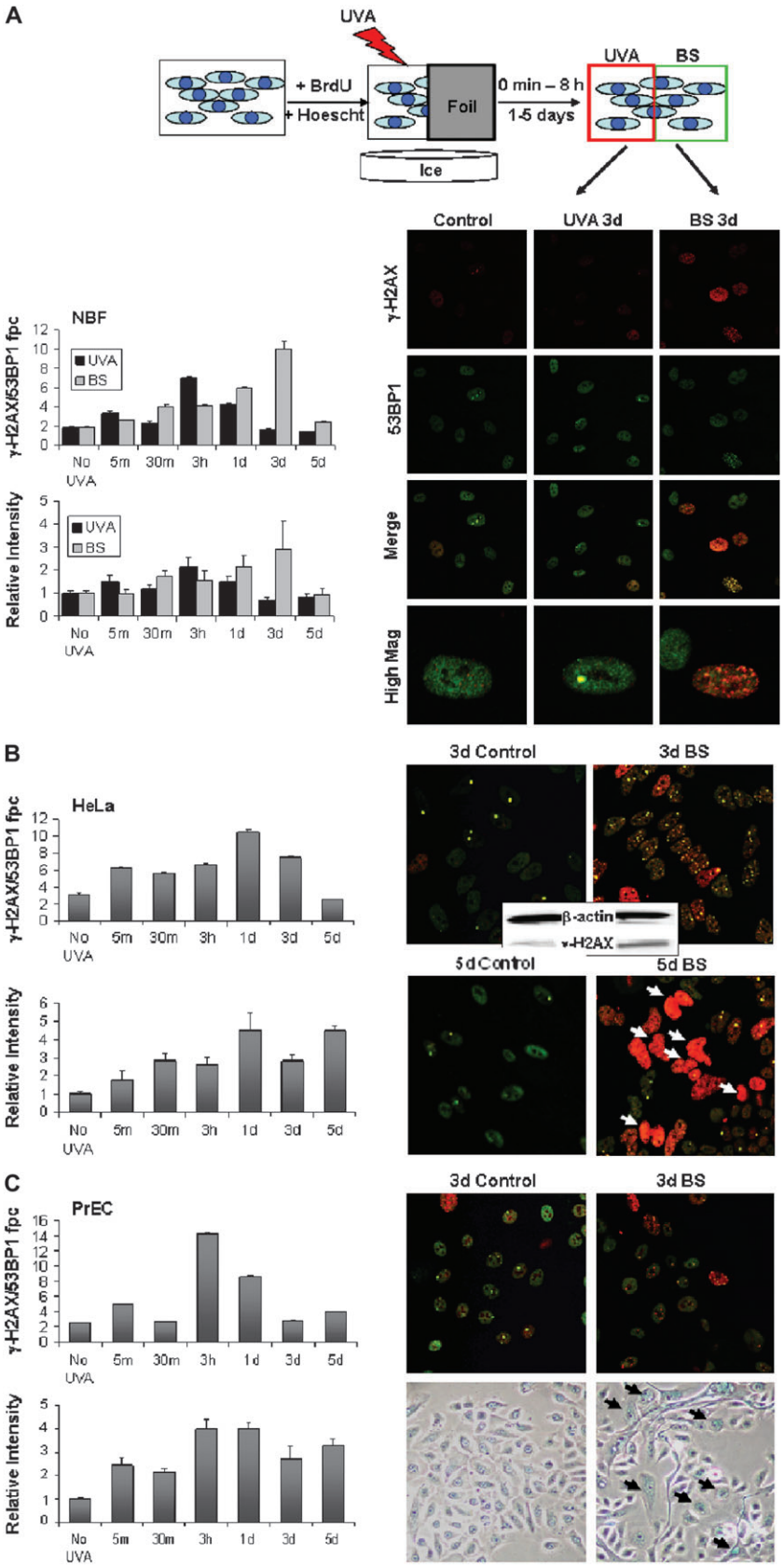

Fig. 1. Exposure of sensitized cells to UVA light induces bystander responses in shielded cells. (**A**) Schematic: cell cultures containing BrdU and Hoechst 3342 were irradiated with 0.04 J/cm^2 UVA with half the culture shielded with foil. After incubation for various periods, foci containing γ-H2AX and 53BP1 were counted in directly exposed and shielded bystander (BS) cells. Total γ-H2AX intensity was also measured. Shown are representative images of NBF cultures taken 3 days after sham exposure (control, left column), direct exposure (UVA 3d, middle column) or shielded from exposure (BS 3d, right column). Cells were stained for γ-H2AX (red, top row) and 53BP1 (green, second row). Merged images (bottom rows) reveal foci double positive for the two proteins. The graphs show values

shielded half confirm that the bystander culture did not receive measurable UVC irradiation (Figure 2A, bottom row).

When examined over a range of moderate UVC doses, NHF bystanders showed increasing amounts of γ-H2AX whether measured by foci numbers or intensity measurements, although the effects were modest with a 2-fold increase 3 h after 20 J/m^2 UVC exposure (Figure 2B). At 20 J/m^2, there was no detectable increase in γ-H2AX/53BP1 focal numbers in the directly exposed cells (supplementary Figure S2 is available at *Carcinogenesis* Online). In the case of HeLa cultures exposed to a strong dose (6000 J/m^2) of UVC, a more substantial bystander effect was seen in the shielded half-culture, with γ-H2AX/53BP1 focal numbers increasing 6-fold over control values at 3 h post-exposure (Figure 2C, left graph). Measurements of γ-H2AX levels in the shielded half-cultures by total relative intensity (Figure 2C, right graph) and by immunoblotting exhibited ∼2-fold increases at 3 h after exposure (Figure 2C, right, inset). These results suggest that damage other DSBs can generate bystander signals that lead to DNA DSBs in neighboring unirradiated cells.

Cell cycle state influences bystander effect vulnerability

In the case of damage induced by IR, previous work has indicated that cells in S phase may be more vulnerable to exhibiting bystander effects (24). In order to examine whether this finding applies to other, non-ionizing, forms of damage, PCNA, a marker of S-phase cells, was used to determine the cell cycle phase of cells in bystander cultures using the UVA protocol (25). For both HeLa cell and NBF cultures, the bystander cells that displayed a robust DNA damage response (>4 fpc) at early time points were also PCNA positive (Figure 3A, yellow arrows, and Figure 3B). While a number of cells lacking PCNA did exhibit bystander effects and some PCNA-positive cells lacked γ-H2AX (Figure 3A, white and red arrows, respectively), these results indicate that in both HeLa and NBF cultures, the strongest bystander DNA damage response is found in S-phase cells, up to 1 day after exposure for HeLa and but only 30 min for NBF. Interestingly, although bystander damage remains elevated several days after exposure, the fraction of PCNA-positive cells decreases (Figure 3B), indicating that bystander damage may preferentially form in S-phase cells, but once formed, the damage remains when these cells exit S phase.

Reactive species and pro-inflammatory cytokines are mediators of the stress-induced bystander effect

The results presented thus far indicate that bystander effects may be a widespread phenomenon occurring when cells are in contact with cells damaged by a variety of initiating factors not limited to IR. In the case of bystander effects induced with IR, several cytokines including tumor necrosis factor alpha, TGF-β and interleukin-8 have been implicated in the propagation of the effect (26,27). In order to further examine whether similar mechanistic pathways may be involved in bystander effects from different cellular stresses, the levels of a number of cytokines involved in inflammation and cellular stress responses were measured in the media of NHFs exposed to UVC light, UVA light after cell sensitization and 0.2 Gy IR, a dose shown to induce notable DNA damage in bystander cells (7). Several factors including tumor necrosis factor alpha, TGF-β, plasminogen activator inhibitor 1 (PAI-1) and insulin-like growth factor 1 were found to be upregulated in the media of stressed NHF cells (Figure 4). These results indicate that the types of cytokines released into the media of primary cells undergoing a variety of stresses are to a large extent independent of the type of stress.

In addition to cytokine production, the propagation of RIBE has been shown to be linked to reactive oxygen species including nitric oxide (NO) (28,29). Previous studies have shown that inhibition of nitric oxide synthase or addition of NO scavengers and other antioxidants can significantly diminish the RIBE (7,13,30). When media from NHF cells damaged with UVC light in the presence of three nitric oxide synthase inhibitors, L-NMMA, 7-NI and AG, as well as the antioxidant tempol was transferred to undamaged NHF cells, all four compounds were found to partially abrogate the bystander increase in γ-H2AX/53BP1 foci numbers (Figure 4B), similar to those found in the RIBE (7). This finding indicates that RIBE and UVC-mediated bystander effects may be propagated by similar factors and that a common mechanism may involve the production of NO and other reactive oxygen species by damaged cells.

In order to verify that NO and cytokines including TGF-β are capable of inducing the DSB response seen in bystander cells, NHF cultures were exposed to NO or recombinant TGF-β in the absence of damage and then examined for γ-H2AX focus formation (Figure 4C). Diethylamine NONOate, which releases NO into aqueous solution (31), is capable of inducing an increase in γ-H2AX focal formation at 10 μM. Likewise, addition of 10 ng/ml TGF-β into fresh media induced γ-H2AX focal formation that is comparable with the DSB induction seen in UVC bystander NHF cell culture (Figure 4C). The addition of both diethylamine NONOate and TGF-β to NHF media did not increase the overall effect, indicating that these compounds may be functioning in the same signaling pathway (data not shown). In order to further investigate the role of TGF-β in this bystander effect, a TGF-β-blocking antibody was added to the media conditioned on NHFs exposed to UVC light and transferred to undamaged NHFs (Figure 4D, left). The blocking antibody abrogated the bystander effect induced by UVC light, whereas a non-specific antibody had no effect. In addition, the blocking antibody also abrogates the increase in γ-H2AX levels induced by the addition of TGF-β (Figure 4D, right). Taken together, these data indicate that NO and TGF-β are capable of inducing a DSB response in cells and are therefore potential signaling molecules of the bystander effect.

Other types of cell stress generate DSBs in bystander and exposed cells

Our findings that DNA DSB generation can be induced in bystander cell populations, not only by IR but also by non-IR radiation, prompted us to examine other sources of environmental stress. Compared with primary cells, tumor cells possess altered cellular metabolism with increased levels of endogenous DNA damage (32). Two unirradiated human tumor cell lines, T406 glioma and HeLa carcinoma, were used to condition media, which then was placed on growing NHF cultures (Figure 5A and B). Exposure of the NHF cultures to conditioned media led to gradual increases in the levels of γ-H2AX/53BP1 foci, reaching a modest but significant 2-fold increase over control values 8 h after media change. These findings indicate that tumor cells may release factors into culture media, which can induce DNA damage in normal cells, and suggest a mechanism by which the presence of tumors might predispose neighboring cells to genomic instability (33).

of colocalized γ-H2AX/53BP1 foci (top left) or total nuclear γ-H2AX intensity (bottom left) per cell for directly irradiated (black bars) and bystander (gray bars) cells at various times post-exposure. Increases in γ-H2AX foci numbers and intensity were statistically significant at 3 h and 1 day in directly exposed cells and from 30 min to 3 days in bystander populations. (**B**) UVA protocol with HeLa cell cultures. Representative images (see panel A) of HeLa control (sham exposed) and bystander cultures taken 3 and 5 days after exposure. Apoptotic nuclei are indicated by white arrows. Immunoblot analysis of control and bystander HeLa cultures 3 days after exposure is shown in the middle inset. The graphs show values of colocalized γ-H2AX/53BP1 foci (top left) or total nuclear γ-H2AX intensity (bottom left) per cell for bystander (gray bars) cells at various times post-exposure. Results were statistically significant for all time points with the exception of 5 days post-exposure in the top left graph. (**C**) UVA protocol with PrEC cultures. Representative images of PrEC control and bystander cultures taken 3 days post-exposure stained for γ-H2AX and 53BP1 (top) or senescence-associated beta-galactosidase, a marker of cellular senescence (bottom). The graphs show values of colocalized γ-H2AX/53BP1 foci (top left) or total nuclear γ-H2AX intensity (bottom left) per cell for bystander (gray bars) cells at various times post-exposure. Results were statistically significant at all time points in intensity measurements and at the 5 min, 3 h, 1 day and 5 day time points in focal counting. Error bars in all graphs indicate the SEM for at least 100 cells.

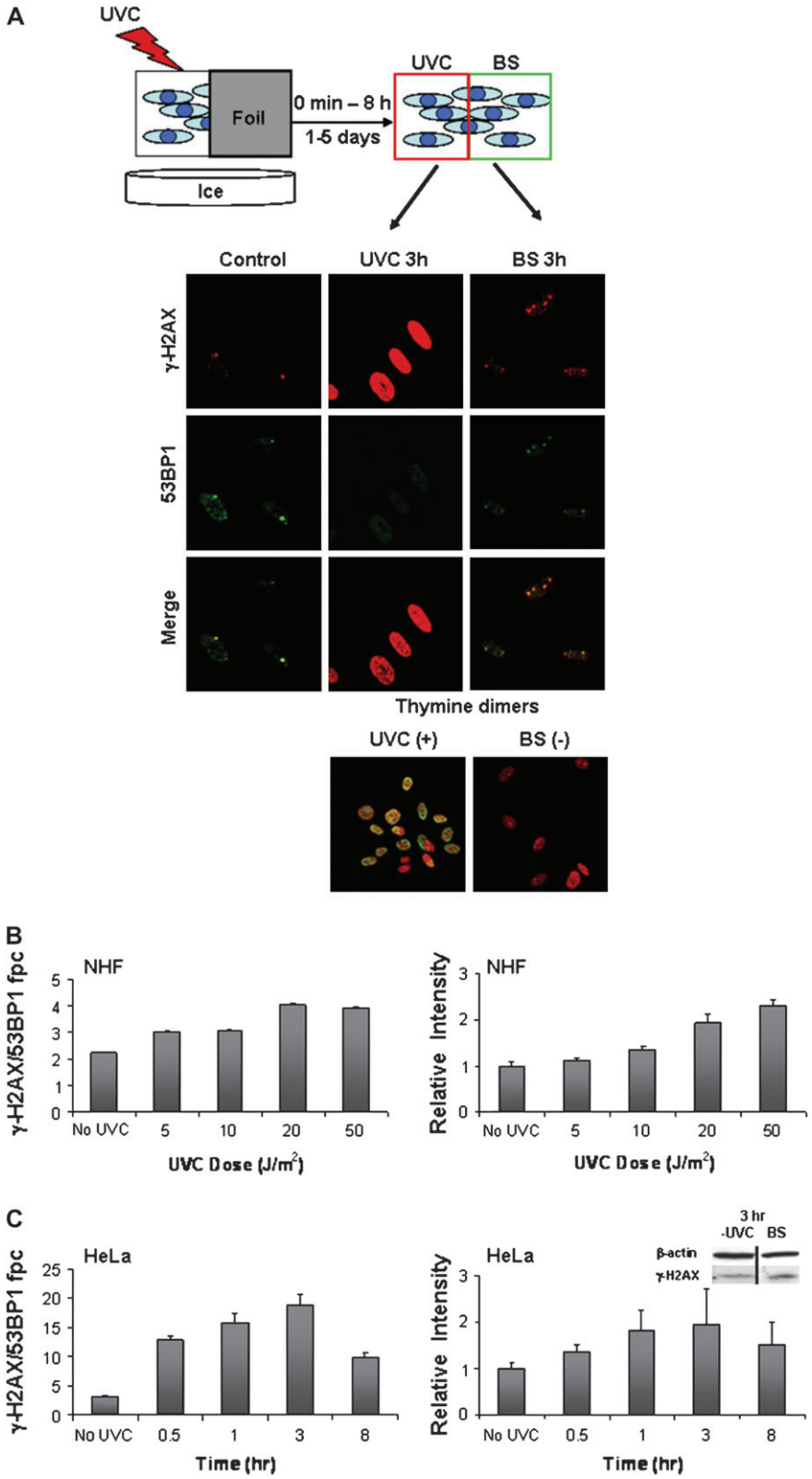

Fig. 2. UVC-induced DNA damage generates bystander responses. (**A**) Schematic: cells were exposed to UVC with half shielded with foil. After incubation, DNA DSBs were assessed in control, irradiated and bystander (BS) cell populations as above. Images are representative of NHF cell cultures 3 h after sham treatment (left column, control), direct exposure to 100 J/m^2 UVC (middle column) or shielding (right column). Cultures were stained for γ-H2AX (red, top row) and 53BP1 (green, second row). Merged images (third row) exhibit yellow foci where the two proteins colocalize. The bottom row images show cells stained for thymine dimers (green) and DNA (red, propidium iodide). UVC-induced photo products are present only in exposed cells. (**B**) Quantification of γ-H2AX induced in NHF bystander cell populations 3 h after various doses of UVC. Colocalized γ-H2AX and 53BP1 fpc (left) and γ-H2AX intensity (right) are shown. Differences in γ-H2AX foci numbers were statistically significant at all doses tested, whereas differences in intensity were significant at the 20 and 50 J/m^2 doses. (**C**) Quantification of γ-H2AX induced in bystander HeLa cell populations various times after 6000 J/m^2 UVC exposure. Colocalized γ-H2AX and 53BP1 fpc (left) and γ-H2AX intensity (right) are shown. All time points tested were significantly different from control levels in both systems. The inset shows immunoblot analysis of control and bystander populations 3 h after irradiation.

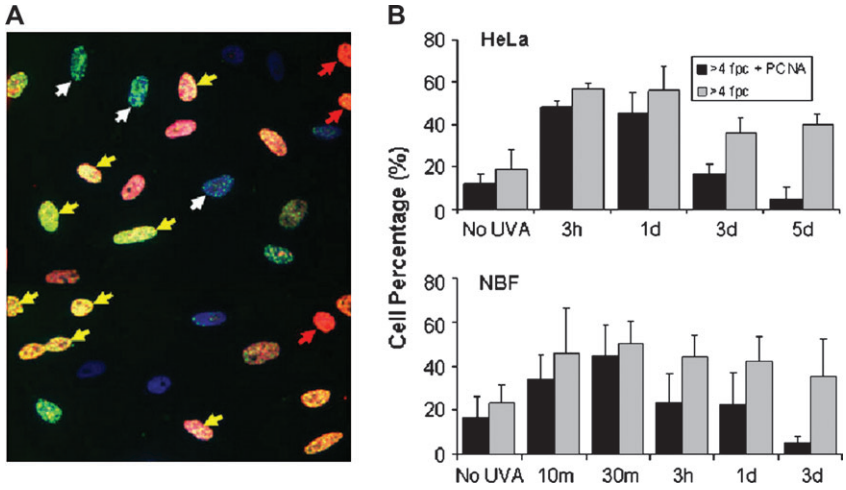

Fig. 3. The role of cell cycle in the bystander effect. (**A**) Image of HeLa bystander cells 3 h after neighboring cell exposure to UVA in the presence of BrdU and Hoechst. γ-H2AX is green, PCNA is red and DNA is blue. Arrows: yellow, cells positive for both γ-H2AX and PCNA; red, cells negative for γ-H2AX and positive for PCNA; white, cells positive for γ-H2AX and negative for PCNA. (**B**) Percentage of bystander cells with >4 γ-H2AX fpc (gray bars) and those cells that were also PCNA positive (black bars) in HeLa (top) and NBF (bottom) cultures. Differences from controls in percentage of cells with >4 fpc were significant at all time points, and differences in the ratio of PCNA-positive versus -negative cells that had >4 fpc were significant at the 3 day and 5 day time points.

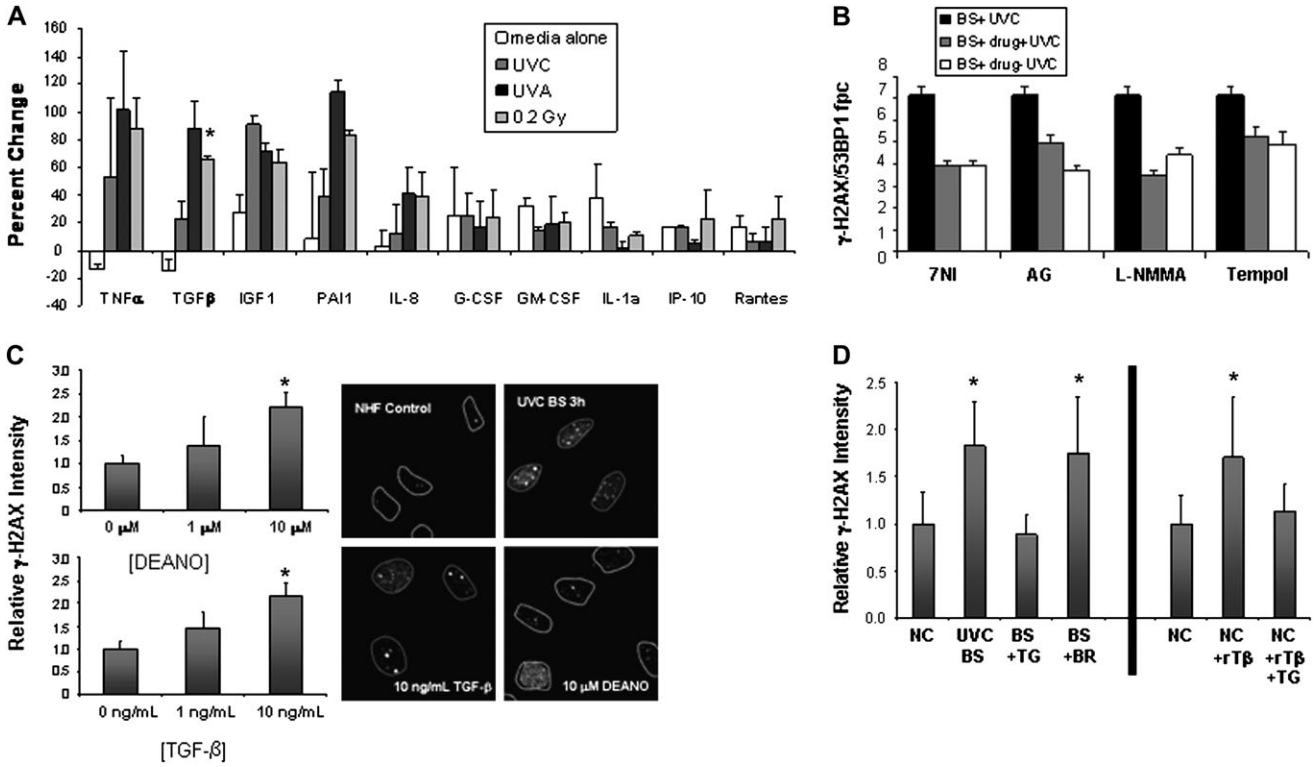

Fig. 4. Cytokines and reactive oxygen species in the bystander effect. (**A**) Cytokines released by damaged cells. Protein levels are compared with the those present in media conditioned on undamaged NHFs. Media-alone (white bars) samples were not conditioned on cells. UVC samples (dark gray) were exposed to 6000 J/m^2 UVC, UVA samples (black bars) were exposed to 0.04 J/m^2 UVA after sensitization with BrdU and Hoechst, 0.2 Gy samples (light gray) were exposed to 0.2 Gy IR. All samples were collected 3 h after exposure. Error bars are the standard deviation for two independent experiments performed 1 week apart. (**B**) Effect of reactive oxygen species and NO modulators on the bystander effect in UVC-irradiated NHFs by media transfer. Colocalized γ-H2AX/53BP1 fpc were measured for bystander (BS) cells in media from NHF cultures that received UVC alone (black), UVC and inhibitor (gray) and bystander cells that received inhibitor alone (white). Inhibitors used were the nitric oxide synthase inhibitors 7-NI, AG and L-NMMA as well as the antioxidant tempol. (**C**) NO and TGF-β can each induce γ-H2AX in otherwise undamaged cells. Various concentrations of diethylamine NONOate, which produces NO (top) or TGF-β (bottom), were incubated with NHFs for 3 h before cells were fixed and analyzed for changes in γ-H2AX relative intensity. The image on the right depicts γ-H2AX formation in undamaged NHFs (top left), in NHF bystander cells 3 h after neighboring cells were exposed to 6000 J/m^2 UVC (top right), NHFs 3 h after exposure to 10 ng/ml TGF-β (bottom left) or 10 μM diethylamine NONOate (bottom right). (**D**, left) The relative γ-H2AX intensity in NHF bystander cells 3 h after UVC exposure without blocking antibody (UVC BS), with a TGF-β blocking antibody (BS + TG) and with a non-specific BrdU antibody (BS + BR). NC denotes normal control NHFs (set to 1.0). (D, right) Normal control cells incubated alone (NC), with recombinant TGF-β protein (NC + rTβ) or with recombinant TGF-β protein plus the blocking TGF-β antibody (NC + rTβ + TG). Data are from at least 100 cells in at least three separate fields. Asterisks in A, C and D indicate significant changes over control values. All compounds shown in (B) significantly reduced the numbers of fpc in bystander cells.

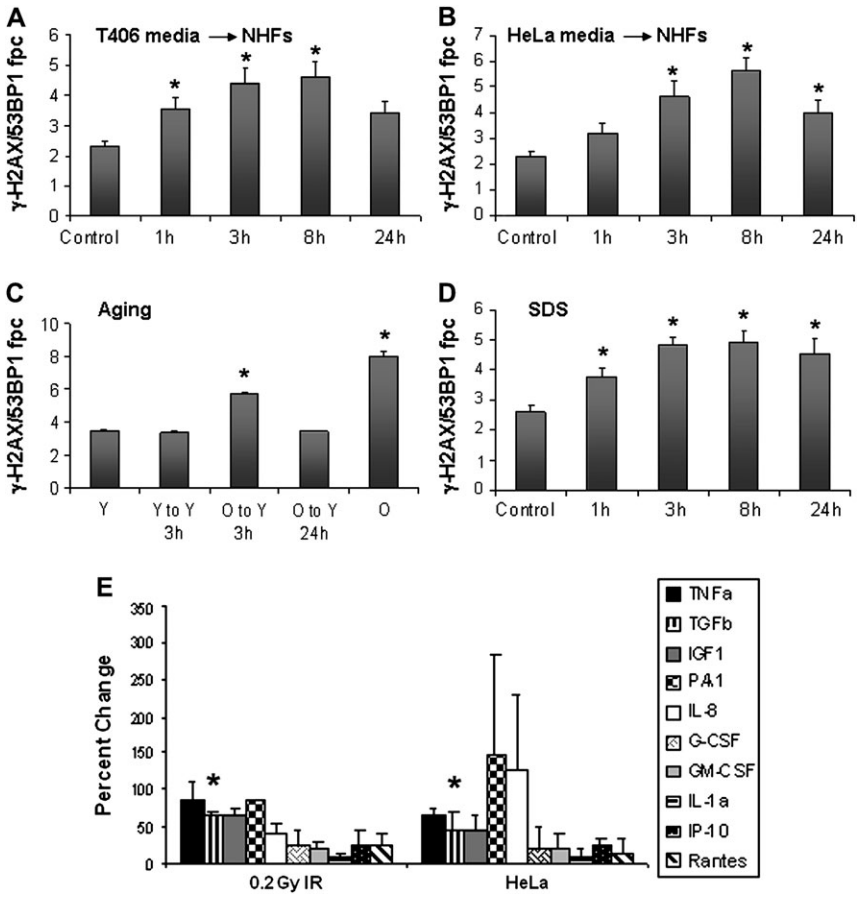

Fig. 5. Undamaged tumor and senescent cells generate a bystander response. Colocalized γ-H2AX/53BP1 fpc were measured for NHFs incubated in media transferred from T406 glioma (**A**) or HeLa cell cultures (**B**). (**C**) Colocalized γ-H2AX/53BP1 fpc in early- (Y) and late-passage NHF cultures (O) and early-passage NHFs incubated in media transferred from early- (Y to Y) or late-passage (O to Y) NHFs. (**D**) Colocalized γ-H2AX/53BP1 fpc were measured for NHFs incubated in the presence of 0.1 mg/ml SDS over time. Error bars in (A–D) represent the SEM for at least 100 cells. (**E**) Tumor cells release cytokines similar to those from damaged primary cells. Media from NHFs exposed to 0.2 Gy IR was compared with that conditioned on undamaged HeLa cells. All media samples were collected 3 h after damage or after 3 h of media conditioning. Error bars are the standard deviation for two independent experiments performed 1 week apart. Asterisks in (A–E) represent statistically significant changes from control values.

Since cells undergoing senescence also harbor increased DNA damage and genomic instability (16), we examined whether media conditioned on late-passage NHFs could produce a bystander effect in early-passage NHFs. Media conditioned on passage 28 (old, 'O') but not on passage 19 (young, 'Y') NHFs generated a modest but significant increase in γ-H2AX/53BP1 focal numbers in recipient passage 19 NHFs (Figure 5C). This increase was transient, peaking 3 h post-media transfer and returning to control levels by 24 h post-transfer. Thus, genetically unstable malignant and senescent cells are capable of inducing a bystander DNA damage response in young, normal primary cell cultures. Taken together, our results indicate the existence of a general cell stress-induced bystander effect. For comparison, we also examined the response of NHFs to a directly administered common irritant, SDS (34). Interestingly, a low concentration of SDS induced γ-H2AX/53BP1 focal formation to an extent similar to those found in some of the bystander protocols (Figure 5D). Media conditioned on HeLa cell cultures also contained a spectrum of elevated cytokine levels similar to that found in media conditioned on damaged NHFs (Figure 5E). These results indicate that bystander damage induced by tumor cells might be induced through similar mechanisms to the RIBE.

Discussion

DNA DSB formation is a well-documented early event in the RIBE [(5,7,35) reviewed in refs. 4,36]. IR causes a significant number of DNA breaks in directly exposed cells, which in turn leads to DSB induction and genomic instability in bystander populations. However, whether this bystander effect is an IR-specific event remained an open question. The results of the present study indicate that IR is not the only signal capable of inducing a DNA damage bystander effect. A substantial DNA DSB response is seen in bystander populations of tumor as well as in primary cells of both epithelial and fibroblast origin in response to non-ionizing DNA damage and cell stress. Other bystander cell responses included apoptosis and senescence depending on cell type.

One relevant question that may arise in bystander studies is that the effect is sometimes rather modest, about 2-fold. However, in stochastic processes, such as damage induced by various types of radiation, small increases in average amounts of DSB damage can lead to relatively large increases in the fraction of cells with greater than a threshold level of DNA damage. In a Poisson distribution model, doubling the average number of fpc from 1 to 2 would lead to a >10-fold increase in cells with >4 foci from 0.4 to 5.3%. Therefore, if a particular adverse outcome is increased at a threshold number of DSBs per cell, small increases in the average DSB frequency make many more cells vulnerable.

Our data show that DSBs are just one type of cellular stressor that can lead to the generation of bystander stress signals, indicating that the bystander effect may be a general response to cell stress mediated, like the RIBE, through the production of reactive oxygen species and pro-inflammatory cytokines. Although this is the first demonstration

of DNA DSB induction in bystander cells to UVC damage, other types of damage such as collagen degradation has been reported when nearby skin cells were exposed to UVC (37,38). In these studies, matrix metalloproteinase-1 was found to be secreted by UVC-damaged keratinocytes. Additionally, matrix metalloproteinase-1 has been implicated in signaling between senescent and normal cells (39). Future work might elucidate what role, if any, matrix metalloproteinase-1 plays in the induction of DSBs in bystander cells. Similarly, this is the first demonstration of PAI-1 induction in damaged normal cells, but its increased expression in cancer cells has also been reported elsewhere (40). In fact, an increased serum level of PAI-1 in cancer patients is an indication of enhanced cancer malignancy. It will be interesting to determine in the future if PAI-1 plays an integral role in bystander signaling. TGF-β has been implicated in the RIBE and has also been shown to inhibit cancer development (30,41). Understanding the interplay of these various factors in cell signaling of DNA damage will provide vital insights into cancer risk and the impact of tumorigenesis on the entire organism.

Interestingly, exposure of normal cells to medium from malignant cultures is capable of giving a bystander response. These data indicate that perhaps cells in communication with tumor cells could have increased DNA damage that could lead to genomic instability (42). This may be especially worrisome when the tumor arises around replicating cells, such as in the gastrointestinal tract or in childhood malignancies. Indeed, understanding the interplay between transformed and non-transformed cells in response to DNA damage may be an important signaling pathway for cancer prevention (43). Recent work indicates, in fact, that senescent and genetically unstable cells may also transmit DNA-damaging bystander signals (44,45). Future studies should address the risk of bystander effects from tumor presence in proximal as well as in distal organs.

Overall, these data indicate that the endogenous levels of DNA DSBs in a cellular population are a good indicator of cellular stress and could serve as a diagnostic marker for alterations in the cellular environment such as cancer and other forms of stress. The model depicted in Figure 6 illustrates how cancers as well as stresses from

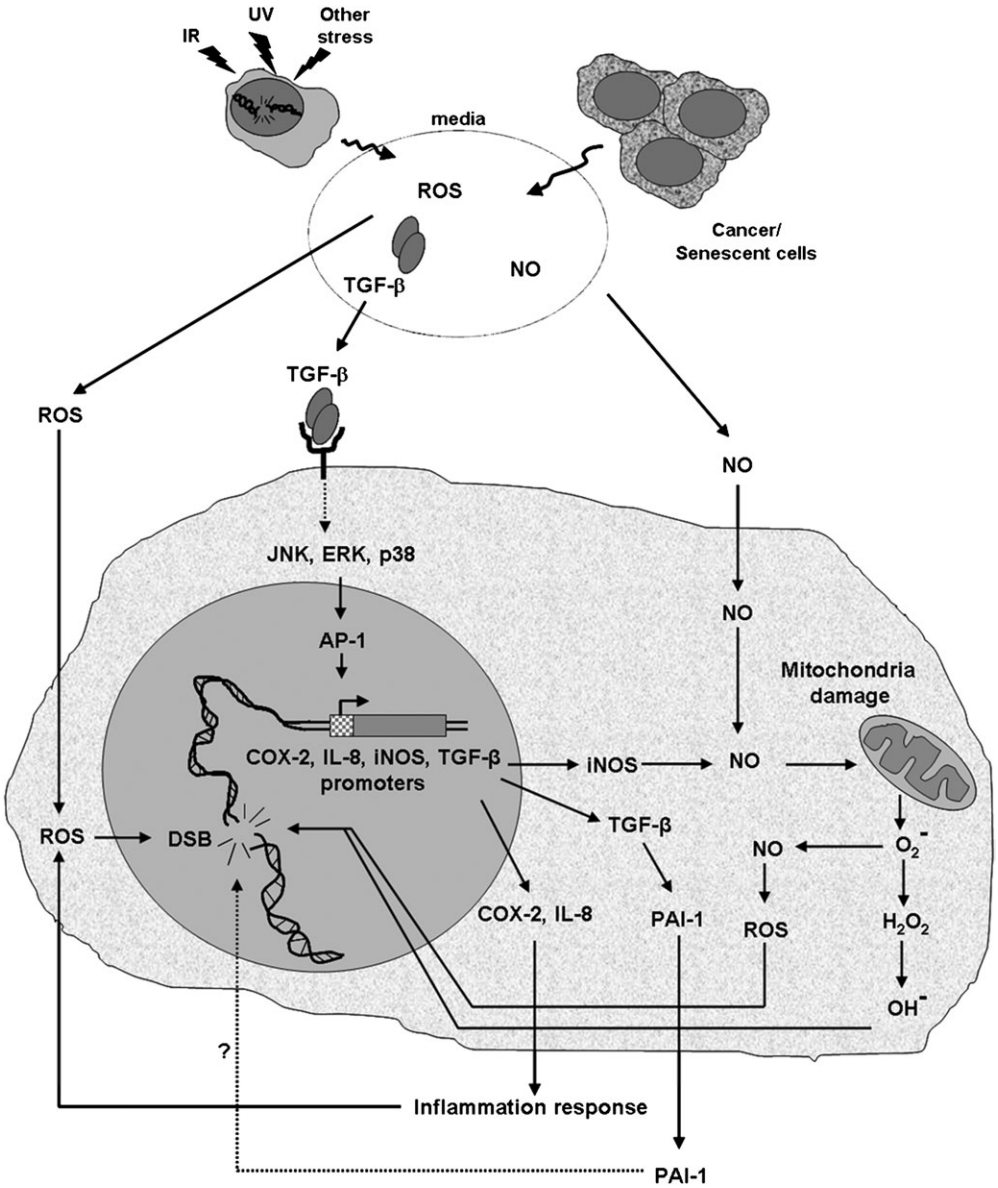

Fig. 6. Model of the bystander stress response. IR, UV rays and stress can all cause DNA damage in cells. This DNA damage or the genomic instability present in tumors leads to the production of reactive oxygen species, NO and TGF-β. All of which could serve to induce a bystander effect in neighboring cell populations. The vulnerable bystander cells display increases in genomic instability, which can be monitored with antibodies to γ-H2AX and other DNA damage proteins.

various other sources including IR, UV and DNA damage itself induces a cell to produce signals that through a variety of pathways (28,30) initiate a DNA damage response in susceptible cell targets. The use of these vulnerable cell populations may be useful in measuring organismal health.

These data also have other implications for the study of stress. While it is well known that chronic inflammatory responses can be pro-oncogenic and stress of various types can cause immune dysfunction leading to long-term health effects, previous work on stress responses has focused on the immediately affected cells and on signal passage through the immune cells (46–49). Perhaps, however, inflammatory stress signals are also passed through non-immune cells (50,51). These non-immune stress signals could have important implications in organismal well-being and in the study of the ability of stress to impact cancer development and progression.

Supplementary material

Supplementary Figures S1 and S2 can be found at http://carcin.oxfordjournals.org/

Funding

Intramural research program of the National Cancer Institute.

Acknowledgements

The authors are grateful to Dr Asako J. Nakamura, National Institutes of Health, for critical reading of this manuscript.

Conflict of Interest Statement: None declared.

References

1. Nagasawa,H. *et al*. (1992) Induction of sister chromatid exchanges by extremely low doses of alpha-particles. *Cancer Res.*, **52**, 6394–6396.
2. Nagasawa,H. *et al*. (2002) Bystander effect for chromosomal aberrations induced in wild-type and repair deficient CHO cells by low fluences of alpha particles. *Mutat. Res.*, **508**, 121–129.
3. Azzam,E.I. *et al*. (2002) Oxidative metabolism modulates signal transduction and micronucleus formation in bystander cells from alpha-particle-irradiated normal human fibroblast cultures. *Cancer Res.*, **62**, 5436–5442.
4. Prise,K.M. *et al*. (2006) What role for DNA damage and repair in the bystander response? *Mutat. Res.*, **597**, 1–4.
5. Hu,B. *et al*. (2006) The time and spatial effects of bystander response in mammalian cells induced by low dose radiation. *Carcinogenesis*, **27**, 245–251.
6. Koturbash,I. *et al*. (2006) Irradiation induces DNA damage and modulates epigenetic effectors in distant bystander tissue in vivo. *Oncogene*, **25**, 4267–4275.
7. Sokolov,M.V. *et al*. (2005) Ionizing radiation induces DNA double-strand breaks in bystander primary human fibroblasts. *Oncogene*, **24**, 7257–7265.
8. Tartier,L. *et al*. (2007) Cytoplasmic irradiation induces mitochondrial-dependent 53BP1 protein relocalization in irradiated and bystander cells. *Cancer Res.*, **67**, 5872–5879.
9. Whiteside,J.R. *et al*. (2009) A bystander effect is induced in human cells treated with UVA radiation but not UVB radiation. *Radiat. Res.*, **171**, 204–211.
10. Bonner,W.M. *et al*. (2008) gammaH2AX and cancer. *Nat. Rev. Cancer*, **8**, 957–967.
11. Limoli,C.L. *et al*. (1993) A new method for introducing double-strand breaks into cellular DNA. *Radiat. Res.*, **134**, 160–169.
12. Limoli,C.L. *et al*. (1995) Photochemical production of double-strand breaks in cellular DNA. *Mutagenesis*, **10**, 453–456.
13. Han,W. *et al*. (2007) Constitutive nitric oxide acting as a possible intercellular signaling molecule in the initiation of radiation-induced DNA double strand breaks in non-irradiated bystander cells. *Oncogene*, **26**, 2330–2339.
14. Rogakou,E.P. *et al*. (1999) Megabase chromatin domains involved in DNA double-strand breaks in vivo. *J. Cell Biol.*, **146**, 905–916.
15. Shimura,T. *et al*. (2007) DNA-PK is involved in repairing a transient surge of DNA breaks induced by deceleration of DNA replication. *J. Mol. Biol.*, **367**, 665–680.
16. Nakamura,A.J. *et al*. (2008) Both telomeric and non-telomeric DNA damage are determinants of mammalian cellular senescence. *Epigenetics Chromatin*, **1**, 6.
17. Adams,M.M. *et al*. (2006) Tying the loose ends together in DNA double strand break repair with 53BP1. *Cell Div.*, **1**, 19.
18. Kashino,G. *et al*. (2004) Evidence for induction of DNA double strand breaks in the bystander response to targeted soft X-rays in CHO cells. *Mutat. Res.*, **556**, 209–215.
19. Smilenov,L.B. *et al*. (2006) A microbeam study of DNA double-strand breaks in bystander primary human fibroblasts. *Radiat. Prot. Dosimetry*, **122**, 256–259.
20. Groesser,T. *et al*. (2008) Lack of bystander effects from high-LET radiation for early cytogenetic end points. *Radiat. Res.*, **170**, 794–802.
21. Ross,C.K. *et al*. (2009) Comments on 'Cellular response to modulated radiation fields'. *Phys. Med. Biol.*, **54**, L11–L33.
22. Pfeifer,G.P. *et al*. (2005) Mutations induced by ultraviolet light. *Mutat. Res.*, **571**, 19–31.
23. Marti,T.M. *et al*. (2006) H2AX phosphorylation within the G1 phase after UV irradiation depends on nucleotide excision repair and not DNA double-strand breaks. *Proc. Natl Acad. Sci. USA*, **103**, 9891–9896.
24. Burdak-Rothkamm,S. *et al*. (2007) ATR-dependent radiation-induced gamma H2AX foci in bystander primary human astrocytes and glioma cells. *Oncogene*, **26**, 993–1002.
25. Moldovan,G.L. *et al*. (2007) PCNA, the maestro of the replication fork. *Cell*, **129**, 665–679.
26. Hei,T.K. *et al*. (2008) Mechanism of radiation-induced bystander effects: a unifying model. *J. Pharm. Pharmacol.*, **60**, 943–950.
27. Ghandhi,S.A. *et al*. (2008) Global gene expression analyses of bystander and alpha particle irradiated normal human lung fibroblasts: synchronous and differential responses. *BMC Med. Genomics*, **1**, 63.
28. Kashino,G. *et al*. (2007) Effective suppression of bystander effects by DMSO treatment of irradiated CHO cells. *J. Radiat. Res. (Tokyo)*, **48**, 327–333.
29. Azzam,E.I. *et al*. (2003) Oxidative metabolism, gap junctions and the ionizing radiation-induced bystander effect. *Oncogene*, **22**, 7050–7057.
30. Shao,C. *et al*. (2008) Role of TGF-beta1 and nitric oxide in the bystander response of irradiated glioma cells. *Oncogene*, **27**, 434–440.
31. Keefer,L.K. *et al*. (1996) "NONOates" (1-substituted diazen-1-ium-1,2-diolates) as nitric oxide donors: convenient nitric oxide dosage forms. *Methods Enzymol.*, **268**, 281–293.
32. Downs,J.A. (2007) Chromatin structure and DNA double-strand break responses in cancer progression and therapy. *Oncogene*, **26**, 7765–7772.
33. Patocs,A. *et al*. (2007) Breast-cancer stromal cells with TP53 mutations and nodal metastases. *N. Engl. J. Med.*, **357**, 2543–2551.
34. Fletcher,S.T. *et al*. (2006) Proteomic analysis of the response of EpiDerm cultures to sodium lauryl sulphate. *Toxicol. In Vitro*, **20**, 975–985.
35. Sedelnikova,O.A. *et al*. (2007) DNA double-strand breaks form in bystander cells after microbeam irradiation of three-dimensional human tissue models. *Cancer Res.*, **67**, 4295–4302.
36. Sokolov,M.V. *et al*. (2007) gamma-H2AX in bystander cells: not just a radiation-triggered event, a cellular response to stress mediated by intercellular communication. *Cell Cycle*, **6**, 2210–2212.
37. Dong,K.K. *et al*. (2008) UV-induced DNA damage initiates release of MMP-1 in human skin. *Exp. Dermatol.*, **17**, 1037–1044.
38. Yarosh,D. *et al*. (2008) UV-induced degradation of collagen I is mediated by soluble factors released from keratinocytes. *Photochem. Photobiol.*, **84**, 67–68.
39. Pawelec,G. *et al*. (2009) Special issue on cancer and ageing. *Mech. Ageing Dev.*, **130**, 1–2.
40. Binder,B.R. *et al*. (2008) The plasminogen activator inhibitor "paradox" in cancer. *Immunol. Lett.*, **118**, 116–124.
41. Zhang,Y. *et al*. (2009) TGFBI deficiency predisposes mice to spontaneous tumor development. *Cancer Res.*, **69**, 37–44.
42. Jungst,C. *et al*. (2004) Oxidative damage is increased in human liver tissue adjacent to hepatocellular carcinoma. *Hepatology*, **39**, 1663–1672.
43. Portess,D.I. *et al*. (2007) Low-dose irradiation of nontransformed cells stimulates the selective removal of precancerous cells via intercellular induction of apoptosis. *Cancer Res.*, **67**, 1246–1253.

44. Coppe,J.P. *et al*. (2008) Senescence-associated secretory phenotypes reveal cell-nonautonomous functions of oncogenic RAS and the p53 tumor suppressor. *PLoS Biol.*, **6**, 2853–2868.
45. Nagar,S. *et al*. (2005) The death-inducing effect and genomic instability. *Radiat. Res.*, **163**, 316–323.
46. Glaser,R. *et al*. (2005) Stress-induced immune dysfunction: implications for health. *Nat. Rev. Immunol.*, **5**, 243–251.
47. Aggarwal,B.B. *et al*. (2006) Inflammation and cancer: how hot is the link? *Biochem. Pharmacol.*, **72**, 1605–1621.
48. Kultz,D. (2005) Molecular and evolutionary basis of the cellular stress response. *Annu. Rev. Physiol.*, **67**, 225–257.
49. Yauk,C. *et al*. (2008) Germ-line mutations, DNA damage, and global hypermethylation in mice exposed to particulate air pollution in an urban/industrial location. *Proc. Natl Acad. Sci. USA*, **105**, 605–610.
50. Zhou,H. *et al*. (2005) Mechanism of radiation-induced bystander effect: role of the cyclooxygenase-2 signaling pathway. *Proc. Natl Acad. Sci. USA*, **102**, 14641–14646.
51. Hei,T.K. (2006) Cyclooxygenase-2 as a signaling molecule in radiation-induced bystander effect. *Mol. Carcinog.*, **45**, 455–460.

Received June 12, 2009; revised July 17, 2009; accepted July 25, 2009